Carbohydrate Polymers 115 (2015) 16–24

Contents lists available at ScienceDirect

Carbohydrate Polymers

journal homepage: www.elsevier.com/locate/carbpol

Development of tannic acid/chitosan/pullulan composite nanofibers from aqueous solution for potential applications as wound dressing

Fenghua Xu[a,1], Baicheng Weng[a,1], Robert Gilkerson[b,c], Luis Alberto Materon[b], Karen Lozano[a,*]

[a] Department of Mechanical Engineering, University of Texas-Pan American, Edinburg, TX 78539, USA
[b] Department of Biology, University of Texas-Pan American, Edinburg, TX 78539, USA
[c] Department of Clinical Laboratory Sciences, University of Texas-Pan American, Edinburg, TX 78539, USA

ARTICLE INFO

Article history:
Received 8 May 2014
Received in revised form 7 August 2014
Accepted 11 August 2014
Available online 2 September 2014

Keywords:
Forcespinning®
Chitosan
Tannic acid
Composite nanofibers
Aqueous solution
Wound dressing

ABSTRACT

This study presents the successful development of biocompatible tannic acid (TA)/chitosan (CS)/pullulan (PL) composite nanofibers (NFs) with synergistic antibacterial activity against the Gram-negative bacteria *Escherichia coli*. The NFs were developed utilizing the forcespinning® (FS) technique from CS-CA aqueous solutions to avoid the usage of toxic organic solvents. The ternary nanofibrous membranes were crosslinked to become water stable for potential applications as wound dressing. The morphology, structure, water solubility, water absorption capability and thermal properties of the NFs were characterized. The ternary composite membrane exhibits good water absorption ability with rapid uptake rate. This novel membrane favors fibroblast cell attachment and growth by providing a 3D environment which mimics the extracellular matrix (ECM) in skin and allows cells to move through the fibrous structure resulting in interlayer growth throughout the membrane, thus favoring potential for deep and intricate wound healing.

1. Introduction

Nanofiber (NF) based structures have shown positive results as three dimensional (3D) scaffolds for cell adhesion and proliferation (Bolin et al., 2009). These artificial 3D nanofibrous structures feature a morphological similarity to the natural extracellular matrix (ECM) in skin, which is characterized by a wide range of pore sizes, high porosity and high mechanical endurance (Kumbar, James, Nukavarapu, & Laurencin, 2008; Pham, Sharma, & Mikos, 2006). Therefore, nanofibrous structures have immense protential as tissue engineering scaffolds for skin substitutes (Min et al., 2004; Rieger, Birch, & Schiffman, 2013), which favor cell adhesion, migration and proliferation (Mattioli-Belmonte et al., 2007). In the last few decades, electrospinning has been the most widely used method to prepare fine fibers (Paneva, Bougard, Manolova, Dubois, & Rashkov, 2008). Recently, forcespinning® (FS) has proven successful as a viable and versatile method to mass produce polymeric fibers. Unlike electrospinning, which draws fibers through the use of electrostatic forces, FS utilizes centrifugal forces which allow for a significant increase in yield, ease of production, and a broader choice of materials to be spun as fibers (Padron, Fuentes, Caruntu, & Lozano, 2013). Both conductive and non-conductive polymer solutions and polymer melts can be spun into fibers without the need of electric fields (Lozano and Sarkar, 2009; Sarkar et al., 2010). As reported, the productivity of this method (over 1 g min^{-1} per nozzle) at the lab scale is significantly higher than lab scale electrospinning (0.3 g h^{-1}) (Ramakrishna, 2005).

Chitosan, the linear cationic (1-4)-2-amino-2-deoxy-β-D-glucan with typical degree of acetylation ca. 0.25, is soluble in certain acidic aqueous solutions, owing to the protonation of the primary amino groups. Chitosan lends itself to a number of chemical reactions, including thermally induced amide formation. All derivatives keep the inherent filmogenicity and antimicrobial activity of plain chitosan. In all fields of study relevant to the administration of chitosan to the human body, chitosan exhibits favorable actions, including immunostimulating activity (Jeong, Kim, & Kim, 2013; Muzzarelli, 2010, 2012; Muzzarelli et al., 2012; Muzzarelli et al., 1990; Qu, Wirsén, & Albertsson, 1999a,b; Ravi Kumar, Muzzarelli, Muzzarelli, Sashiwa, & Domb, 2004). However, due to the strong intermolecular interaction of CS macromolecules, it is difficult to directly spin pure chitosan (Ohkawa, Cha, Kim,

* Corresponding author. Tel.: +1 956 6657020; fax: +1 956 6653527.
E-mail address: lozanok@utpa.edu (K. Lozano).
[1] The authors contributed equally to this work.

http://dx.doi.org/10.1016/j.carbpol.2014.08.081
0144-8617/

Nishida, & Yamamoto, 2004). In order to improve the fiber forming ability of CS and expand its potential applications, CS is commonly blended with other polymers that possess fiber forming capabilities such as polyethylene oxide (PEO) (Desai, Kit, Li, & Zivanovic, 2008; Pakravan, Heuzey, & Ajji, 2011), polyvinyl alcohol (PVA) (Jia et al., 2007; Ohkawa et al., 2004), polylactic acid (PLA) (Xu et al., 2009), silk fibroin (Park, Jeong, Yoob, & Hudson, 2004) and collagen (Chen, Mo, & Qing, 2007), which are all biocompatible and biodegradable and will not restrict the final applications of CS NFs.

Pullulan (PL) is a neutral linear, fungal exopolysaccharide consisting of α-1,6-linked maltotriose residues, produced from starch by *Aureobasidium pullulans* (Yuen, 1974). Besides the common advantages of natural polysaccharides, such as non-toxic, biocompatible and biodegradable, the distinctive linkage pattern of PL endows it with unique physical properties, including excellent water solubility, high-water-absorbing capability, adhesive properties and the capability to form strong resilient films and fibers (Li et al., 2011; Singh, Saini, & Kennedy, 2008). The PL films and fibers are edible, colorless, tasteless, odorless, flexible, and possess excellent mechanical properties (Kristo, Biliaderis, & Zampraka, 2007). PL can be easily molded and has been proven effective for fiber formation (Singh et al., 2008). Recently PL is being investigated for several biomedical applications such as targeted drug and gene delivery (Rekha & Sharma, 2009), tissue engineering (Na, Shin, Yun, Park, & Lee, 2003), wound dressing (Li et al., 2011) to mention some.

Tannic acid (TA) is a gallic ester of D-glucose in which the hydroxyl groups of the carbohydrate are totally esterified with gallic acid dimers. Its multiple phenolic groups can interact with biological macromolecules (Aelenei, Popa, Novac, Lisa, & Balaita, 2009). TA possesses strong astringent, antioxidant, hemostatic and antibacterial properties and therefore besides others uses in the textiles, wine, and wood industries, it has found beneficial applications in the medical area as a drug for the treatment of skin ulcers, burns, wounds and toothache. It is expected that the addition of TA to other biomaterials will synergistically enhance healing properties.

In this study, we mass produced CS/PL binary composite NFs from a CS citric acid (CA) aqueous solution using FS technique. The aqueous solution was applied not only to avoid the trace presence of the toxic organic solvents in the produced fibers but also to promote the development of functional fibers containing water-soluble drugs for wound dressing applications. The drug, TA was then incorporated fabricating water-stable TA/CS/PL ternary composite NFs through subsequent crosslinking. The morphology, structure, water solubility, water absorption capability, and thermal properties of the NFs were characterized. The antibacterial activity of the ternary composite NFs against gram-negative bacteria, *Escherichia coli* was investigated. The biocompatibility and the potential applications of these fiber membranes as wound dressing was evaluated in vitro with mouse embryonic fibroblasts (NIH 3T3).

2. Experimental

2.1. Materials

Pullulan was purchased from Tokyo Chemical Industry Co. (Japan). Low molecular weight Chitosan (M_w = 50,000–190,000 and 75–85% degree of deacetylation), tannic acid (produced from Chinese natural gall nuts) and citric acid were purchased from Sigma–Aldrich. Anhydrous potassium bromide (KBr, >99%) was purchased from Fisher Sci. Deionized water (DI water, 18 MΩ cm) was produced from Mill-Q (Millipore Ltd., UK).

2.2. Preparation of the solutions

The 3 wt% CS-CA salt solution was prepared by dissolving chitosan in citric acid aqueous solution, and then allowing the solution to stir overnight. PL (18 wt%) was added into CS-CA solution and continuously stirred at room temperature until the solution became clear. TA (1 wt%) was then added into the solution, and stirring continued until it became clear.

2.3. Production of NFs

FS was performed on a lab scale Cyclone™ L-1000M (manufactured by FibeRio Technology, Corp.). Work reported in the literature has shown the schematics of the FS system as well as detailed description of the theory and experimental processes (Padron et al., 2012, 2013; Raghavan, Soto, & Lozano, 2013; Sarkar et al., 2010; Weng, Xu, & Garza et al., 2014; Weng, Xu, & Lozano, 2014; Weng, Xu, Salinas, & Lozano, 2014). A cylindrical spinneret equipped with 30 gauge half-inch regular bevel needles (Becton, Dickinson and Company) was selected; 2 mL of the prepared polymer solution were injected into the spinneret using a 5-mL plastic syringe. The polymer solution was extruded through the orifices by centrifugal force and fiber jets were formed. Fibers were collected either by utilizing a deep-dish fiber collector with equally distanced vertical pillars or by allowing the fibers to deposit on a polypropylene substrate. After collection, the fibers were covered and stored under desiccation.

2.4. Crosslinking of the FS membranes and stability test

The TA/CS/PL composite membranes were cured in an oven at 150 °C for at least 1 h to induce chemical crosslinking with CA. After crosslinking, the composite NFs were immersed in DI water for 48 h. Then the samples were dried under ambient conditions prior to analysis.

2.5. Characterizations of NFs

A field emission scanning electron microscopy (FE-SEM; Sigma VP Carl Zeiss, Germany) was used to analyze fiber morphology, homogeneity, orientation, and fiber size. The average diameter of the NFs was analyzed by randomly measuring 300 different NFs from the SEM images using the image analysis software (JMicroVision V.1.2.7, University of Geneva, Geneva, Switzerland).

Fourier transform infrared spectroscopy (FTIR) measurements were performed on a Bruker IFS 55 Equinox FTIR spectrometer. The FTIR spectra were recorded from KBr pellets in the range of 4000–400 cm^{-1}.

X-ray diffraction (XRD) studies were conducted on a Bruker-AXS D8 advance X-ray diffractometer using a Cu Kα radiation source filtered with a graphite monochromator (λ = 1.5406 Å). ^1H nuclear magnetic resonance (NMR) measurement was carried out on a Bruker DRX600 600 MHz nuclear magnetic resonance spectrometer at 25 °C. 10 mg of the ternary composite NF membrane before crosslinking were dissolved in 0.75 mL deuterium oxide and loaded into the NMR rotor at external magnetic field strengths of 14.1 T.

Thermo-physical analysis was conducted through thermogravimetric analysis (TGA) and differential scanning calorimetry (DSC). Both TGA and DSC instruments are from the TA-Q series, model TGA-Q500 and DSC-Q100 (TA Instruments Inc.), respectively. For TGA, 10 mg samples were heated on platinum pans from room temperature to 600 °C at a heating rate of 5 °C min^{-1} under air and nitrogen flow (30 mL min^{-1}). For DSC, samples of about 10 mg were sealed in aluminum pans and heated from room temperature to 200 °C at a heating rate of 1 °C min^{-1} under 30 mL min^{-1} of air flow, and then cooled to room temperature again at the same rate.

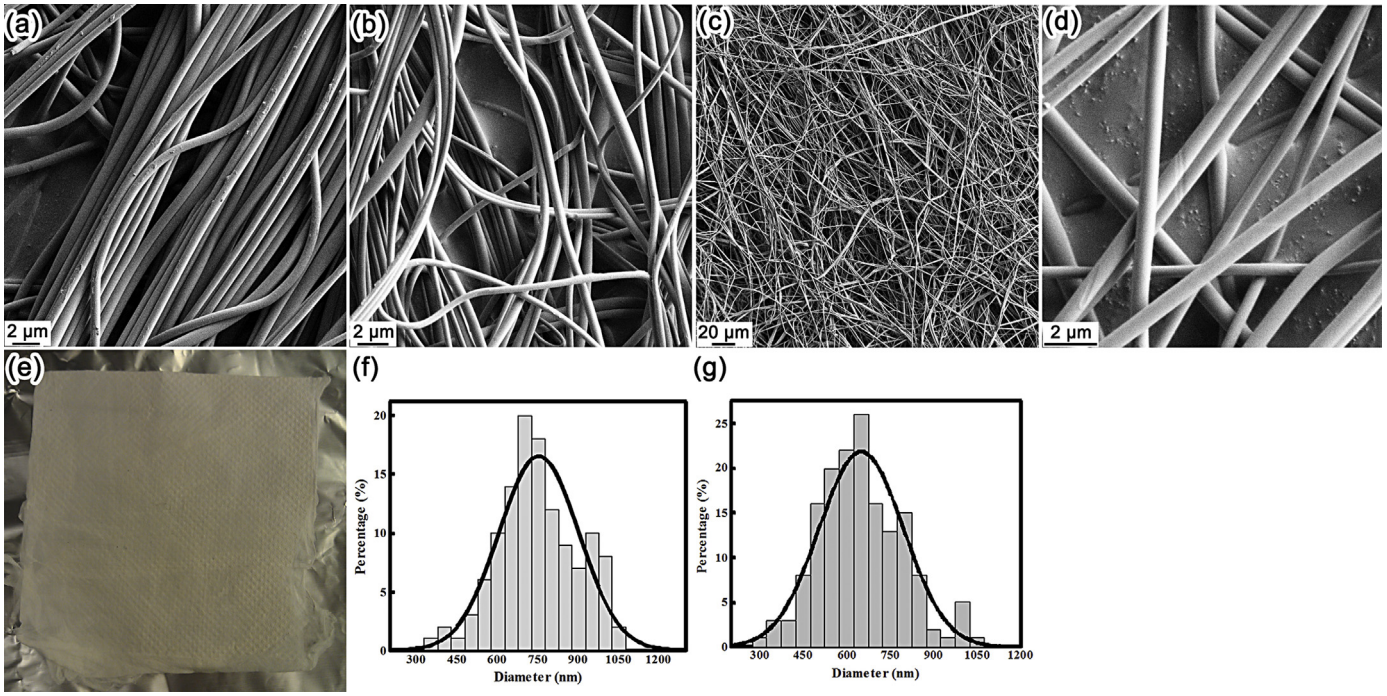

Fig. 1. (a) SEM images of pure PL NFs, (b) CS/PL composite NFs, and (c) TA/CS/PL composite NFs. (d) SEM picture of a magnified image of (c). (e) Photograph of a nonwoven ternary composite membrane. (f) and (g) Graphs representing the diameter distributions of pure PL and ternary composite NFs, respectively.

Water absorption capability of the composite nanofibrous membrane was investigated by soaking the dried sample in DI water at room temperature for 1 h. Water on the surface of the membranes was then wiped off with tissue paper, and the weight of the samples was determined. The water absorption capability (%) of the membranes was calculated using the following equation:

$$\text{Water absorption}\,(\%) = \left[\frac{W - W_0}{W_0}\right] \times 100,$$

where W_0 and W represent the weight of the sample before and after immersion in water, respectively.

2.6. Antibacterial activity

To perform the antibacterial testing, the viable cell counting method was used against Gram-negative *Escherichia coli* ATCC 25922 (*E. coli*) which is commonly found on wounds, and causes wound infections. Samples of about 100 mg were placed into 10 mL of the bacteria/tryptic soy broth, followed by incubation in a shaker at room temperature for 24 h. Then, 100 μL of the bacterial broth was spread onto agar plates. The number of colonies was then counted on agar plates after the 24 h incubation at 37 °C compared to the control that had not been exposed to the fibers.

2.7. Cell culture

To study cell behavior, morphology, attachment and spreading, NIH 3T3 mouse embryonic fibroblast cells (kind gift of Eric Schon, Columbia University) were investigated on the ternary nanofibrous membranes. The result was compared to the control of NIH 3T3 cells grown on glass coverslips. Cells were cultured in Dulbecco's Modified Eagle's Medium (DMEM) supplemented with 10% fetal bovine serum (FBS), 100 IU mL^{-1} penicillin and 100 μg mL^{-1} streptomycin, and maintained at 37 °C in a humidified incubator with 5% CO_2. The ternary composite membranes were placed into a 6-well cell culture plate and then sterilized under UV light for 20 min, followed by washing with phosphate-buffered saline (PBS). The cells were seeded onto the membranes, and cultured for 1, 3, 5 and 7 days. After incubation, the cells were stained with 40 nM MitoTracker Red CMXRos in growth medium for 20 min at 37 °C. After that, the cells were rinsed twice with PBS, and subsequently fixed with 4% paraformaldehyde in PBS at 4 °C for 30 min, followed by staining with 300 nM 4′,6-diamino-2-phenylindole (DAPI) for 5 min. Being washed 3 times with PBS after staining and mounted with 50% glycerol in PBS, the cells were viewed and analyzed using on an Olympus FV10i confocal laser-scanning microscope.

3. Results and discussion

3.1. Morphology of NFs

The development of pure PL NFs (Fig. 1a) utilizing the FS technology was established given that PL was used as the carrier to promote fiber formation for CS. CS was dissolved in citric acid solution generating a corresponding CS-CA salt solution, given the protonation of free amino groups along the polymer chain. This salt solution was then mixed with the PL without the use of organic solvents and CS/PL binary composite NFs were developed, as shown in Fig. 1b. TA was then incorporated and TA/CS/PL composite NFs were obtained. The color of the NFs changed from white to a light brown due to the addition of TA. Fig. 1c and d shows SEM images of the developed ternary composite NFs whereas Fig. 1g displays their diameter distribution. The ternary composite NFs produced by FS exhibit a smooth, long and continuous morphology with 650 nm in average diameter and a standard deviation of 145 nm, which is smaller than that of pure PL NFs (750 ± 150 nm) (as shown in Fig. 1f). The average diameter of fibers and diameter distribution were calculated using an image analysis software, the diameters of at least 300 fibers per sample with random image sampling were measured. The developed NFs could be further pressed or deposited on a polypropylene substrate to achieve desirable properties (such as porosity, thickness, etc.). Fig. 1e shows the 8 cm × 8 cm × 100 μm (length by width by thickness) nonwoven ternary composite membrane.

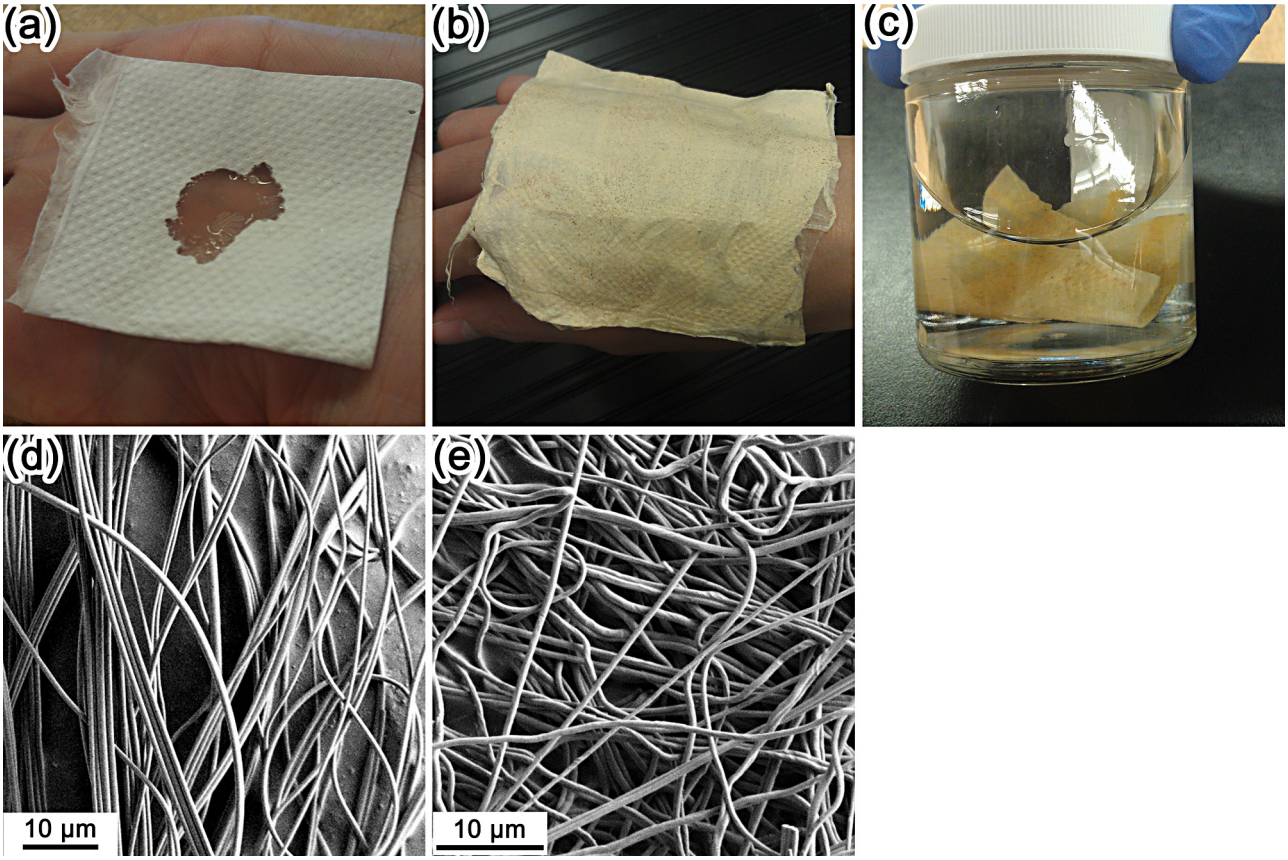

Fig. 2. Photographs of water stability of ternary composite membrane before (a) and after (c) crosslinking. The crosslinked membrane is stable in water, while the non-crosslinked membrane can be dissolved and damaged by a drop of water. (b) Presents a conformal and flexible crosslinked ternary membrane deposited on a hand. (d) Shows an SEM image of the crosslinked ternary membrane. (c) and (e) Show a photograph and SEM image of the crosslinked ternary composite membrane after immersion in water for 48 h.

3.2. Crosslinking of NFs

PL and CS are highly hydrophilic, therefore present poor stability in water, even a drop of water on the composite membrane can dissolve and destroy the nanofibrous membrane (Fig. 2a). Therefore, molecular crosslinking was conducted to ensure prolonged structural integrity for potential application as wound dressing materials. The ternary composite membranes were cured in an oven at 150 °C induce chemical crosslinking via CA present in the system. The curing temperature was selected according to results obtained from TGA and DSC analysis. After crosslinking, the color of the ternary composites became yellowish (Fig. 2b), and the membrane was as flexible and conformal as it was before crosslinking, therefore suitable for irregular and intricate wounds. Fig. 2d shows the typical SEM image of crosslinked composite NFs. The stability in water of the crosslinked NF membranes was then analyzed by immersing it in water for 48 h (Fig. 2c), no changes were observed as it can be seen in the SEM micrographs shown in Fig. 2e.

3.3. FTIR, XRD and ^{1}H NMR measurements

Fig. 3A shows the FTIR spectra of pure PL NFs, composite NFs, CS and TA powder. In the spectrum of pure PL NFs, the absorption around 850 cm^{-1} characterizes the α-configuration of α-D-glucopyranose units. Absorption at 755 cm^{-1} demonstrates the presence of α-(1, 4) glucosidic bonds, and band at 929 cm^{-1} proves the presence of α-(1,6) glucosidic bonds (Karim et al., 2009). The prominent band at 3403 cm^{-1} is attributed to the O—H stretching vibration. The band at 2925 cm^{-1} is due to stretching vibrations of CH and CH_2 groups. Absorption at 1640, 1368 and 1152 cm^{-1} is assigned to O—C—O stretching vibrations, C—O—H bending motion, and C—O—C stretching vibrations, respectively, which is consistent with the reported literature (Cheng, Demirci, & Catchmark, 2010; Singh and Saini, 2007).

In the CS/PL binary composites, absorption at 1727 cm^{-1} is ascribed to the C=O stretching vibration which may be the result of a coalescence peak of the ester carbonyl bond and carboxyl C=O groups in CA (Shi et al., 2008). The absorption peaks at 1384 cm^{-1} and 1080 cm^{-1} correspond to CH_3 deformation and C—N bending vibration, respectively (Azlan, Wan Saime, & Lai Ken, 2009) and are found to be the same as that in the CS powder spectrum. Furthermore, the absorption peak at 850 cm^{-1} in the PL NFs attributed to α-glucopyranose units decreases, which may result from the incorporation of CS with β-glycosidic bonds observed at 896 cm^{-1} in the CS powder spectrum. The results suggest that CS-CA was homogenously dispersed and distributed within the composite (Jia et al., 2007).

Compared to the CS/PL binary composites, the absorption peak at 1727 cm^{-1} observed in the TA/CS/PL composite NFs and ascribed to the C=O stretching vibration increases significantly. This increment results from the incorporation of TA, which has a large number of ester bonds. Moreover, absorption at 1612 and 1535 cm^{-1} are attributed to the aromatic C=C peaks of TA (Can, Bulut, Örnek, & Özacar, 2013; Can, Bulut, & Özacar, 2012; Kim and Kim, 2003; Mohammed-Zieglera & Billes, 2002). These results fully illustrate that TA was molecularly dispersed in the ternary composites. The spectra of these membranes before and after heat treatment are quite similar. However, absorption peak at

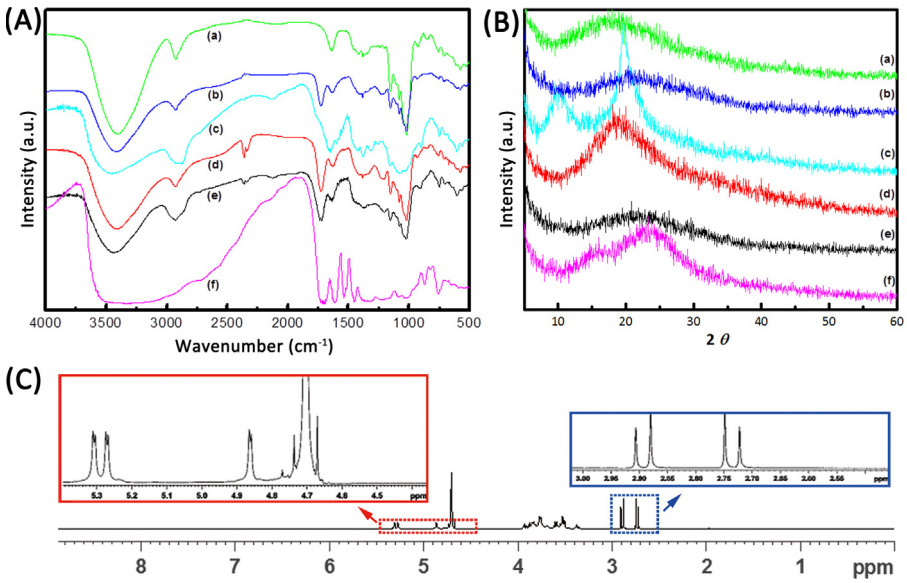

Fig. 3. (A) FTIR spectra and (B) XRD patterns of (a) pure PL NFs, (b) binary composite NFs, (c) CS powder, (d) ternary composite NFs, (e) crosslinked ternary composite NFs, and (f) TA powder. (C) ^{1}H NMR spectrum of the ternary composite NFs.

2925 cm^{-1}, ascribed to stretching vibrations of CH and CH_2 groups becomes broader as a result of the reaction of the carboxyl groups from CA with hydroxyl groups from the PL and amino groups from the CS (Shi et al., 2008).

Fig. 3B illustrates the XRD patterns of pure PL NFs, composite NFs, CS and TA powder. For pure PL NFs, there is a broad peak posited around 18°. With the addition of CS-CA, the diffraction peak shifts to around 21°, the relative peak intensity decreases and the crystalline peaks of citric acid are not observed. The observations indicate that CS-CA was homogenously and molecularly dispersed in the composite NFs, resulting in the deformation of the lattice structure. With further addition of TA, the composite NFs exhibit a more crystallized peak at about 19°, compared to the binary composite. After crosslinking, the relative intensity of this peak decreases. This completely amorphous structure probably results from the covalent reactions between CA with PL and CS. The XRD results demonstrate the effect of CS and TA in the composite NFs. Furthermore, ^{1}H NMR measurement of the ternary composite NFs was conducted. The ^{1}H NMR spectra (Fig. 3C) show characteristic peaks of the glucosamine residues of CS around 4.65 ppm corresponding to the proton bonded to the anomeric carbon-1, and around 2.9 ppm corresponding to the proton bonded to carbon-2 (de Abreu and Campana-Filho, 2005; Rocasalbas, Touriño, Torres, & Tzanov, 2013). The peaks around 2.73 ppm are attributed to the methylene protons of CA (Yang, Webb, & Ameer, 2004), while the peaks from 5.2 to 5.4 ppm are ascribed to the protons of phenol groups from TA (McMurry, 2010, chap. 13).

3.4. Thermo-physical characterizations

Fig. 4A and B shows TGA curves with their corresponding derivative weight loss curves for PL and composite NFs at a ramping speed of 5 °C min^{-1} in a nitrogen atmosphere. The thermogram for the pure PL NFs exhibits a typical thermal degradation behavior of polysaccharides, with the onset degradation temperature about 250 °C and a maximum decomposition rate around 306 °C. Both CS/PL binary and TA/CS/PL composite NFs have the first mass loss with maximum rate at 150 °C, which is a result of the evaporation of water produced during the covalent crosslinking of carboxyl groups of CA, hydroxyl groups of PL and amino groups of CS in the composites. For verification purposes, it can be observed that the post-heated (crosslinked) NFs membranes do not show this mass loss. Composite NFs have an obviously different degradation behavior from pure PL NFs due to the formation of the covalent bonds by the crosslinking mechanism. Both composite NFs show quite unstable thermal stability with onset degradation at about 185 °C, which is significantly lower than the onset decomposition temperature of pure PL NFs (about 250 °C). The slope of the TGA curves for the composites is also lower than that of pure PL during degradation. Furthermore, there is a difference in the residual weight of the different systems. At 600 °C, PL has a residue of ~11%, the binary composite of ~16% and the ternary composite of ~14%. This further indicates that with the successive addition of CS-CA salt, and TA, the thermal behavior of the composite NFs changes.

Fig. 4C and D shows the TGA curves and the derivative weight loss curves in an air atmosphere, it is observed that the composite NFs have similar weight loss with maximum rate around 150 °C as those observed in a nitrogen atmosphere. In the case of the composite NFs, the onset decomposition temperature decreased by about 65 °C compared to pure PL NFs. At temperatures higher than 300 °C, the ternary composite NFs appear more unstable than the binary composite NFs. These results indicate that the incorporation of CS-CA and TA caused notable changes in the thermal properties of the developed NFs as observed in the TGA analysis under a nitrogen atmosphere. Fig. 4E exhibits the DSC analysis carried out under air atmosphere with a temperature ramp of 1 °C min^{-1} and up to 200 °C. The composite NFs show an endothermic peak around 150 °C, while the pure PL and the post-heat (crosslinked) composite NFs do not exhibit this endothermic peak at this temperature range.

3.5. Water absorption capability of the membrane

The water absorption capability is one of the most important properties of the membrane for wound dressing, because a desirable wound dressing must absorb excess exudates without leakage to its surface (Zahedi, Rezaeian, Ranaei-Siadat, Jafari, & Supaphol, 2010). The water absorption capacity of the ternary composite membrane was assessed by immersing the membrane in water at room temperature for 1 h. Its water absorption capacity was higher than 400%. This result shows that the ternary composite membrane has good water uptake ability without compromising its structure.

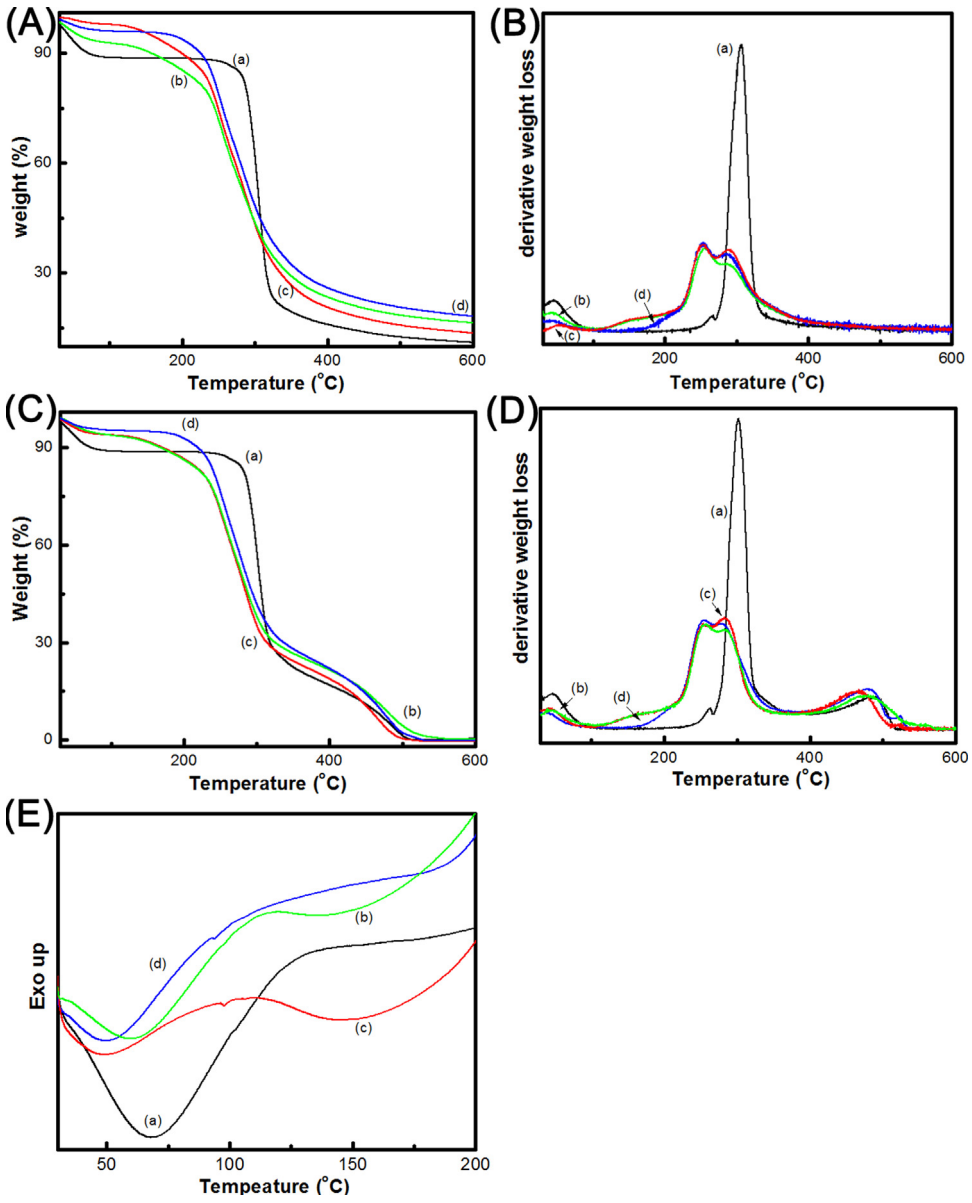

Fig. 4. TGA curves in nitrogen (A) and air (C) atmosphere and DSC curves (E) in air atmosphere of (a) pure PL NFs, (b) binary composite NFs, (c) ternary composite NFs, and (d) crosslinked ternary composite NFs. (B) and (D) are the derivative weight loss curves of TGA data from (A) and (C), respectively.

Rapid water uptake rate was also observed. This could be attributed to the high hydrophilicity of both PL and CS, resulting in water diffusing very rapidly through these materials (Baskar & Sampath Kumar, 2009). Furthermore, it was noted that the developed membranes did not give off the absorbed water and were able to retain most of it within the membranes, this behavior is considered crucial for wound dressing applications (Li et al., 2011). Effective wound dressings must be able to maintain a prolonged moist microenvironment to benefit the epithelialization of wound while preventing the formation of the scab (Winter, 1962).

3.6. Antibacterial assessment

As already shown in the literature, CS provides inhibition of many microbes. The mechanism by which CS exerts its antimicrobial action has not been fully explained, but the antibacterial activity of CS is mainly based on the damaging interaction of the polycation (protonated amino groups) with the negatively charged surfaces of bacteria, resulting in loss of membrane permeability, cell leakage, and finally cell death (Hang, 2010; Helander, Lassila, Ahvenainen, Rhoades, & Roller, 2001; Ignatova, Starbova, Markova, Manolova, & Rashkov, 2006). Moreover, on the antimicrobial activity, TA inhibits bacterial growth as proven for *E. coli*, *Staphylococcus aureus* and *Pseudomonas aeruginosa*, etc. (Çolak, Yapici, & Yapici, 2010). Its antimicrobial activities include inhibition of extracellular microbial enzymes, deprivation of the substrates required for microbial growth, or direct action on microbial metabolism through inhibition of oxidative phosphorylation (Scalbert, 1991). The effect of the ternary composite NFs combining CS and TA against *E. coli* growth was evaluated using the viable cell counting method and compared to the control obtained by incubating *E. coli* in broth without fibers. As shown in Fig. 5, the culture containing the ternary composites resulted in a complete inhibition of *E. coli* growth showing that the developed combination of materials effectively promoted fiber formation while successfully achieving the needed antimicrobial activity.

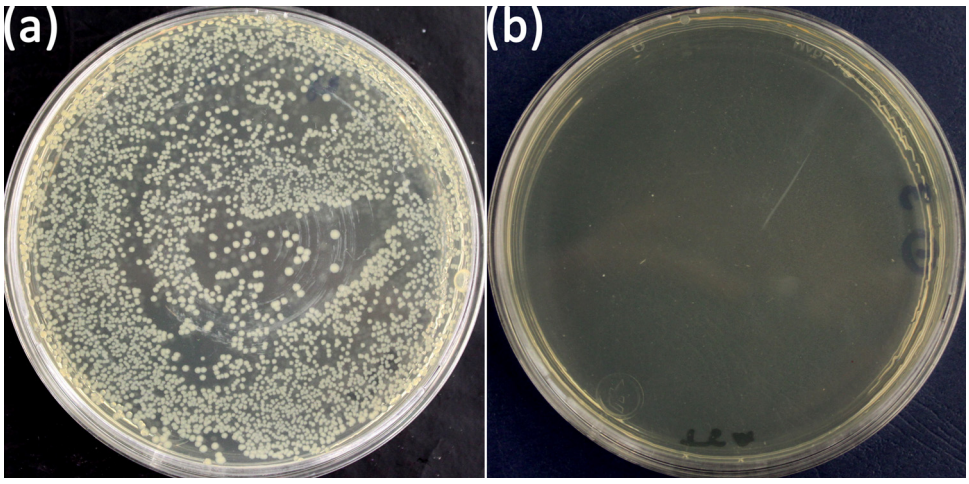

Fig. 5. The antibacterial activity against *E. Coli* of (a) control sample by incubating bacteria in broth without samples and (b) ternary composite NFs.

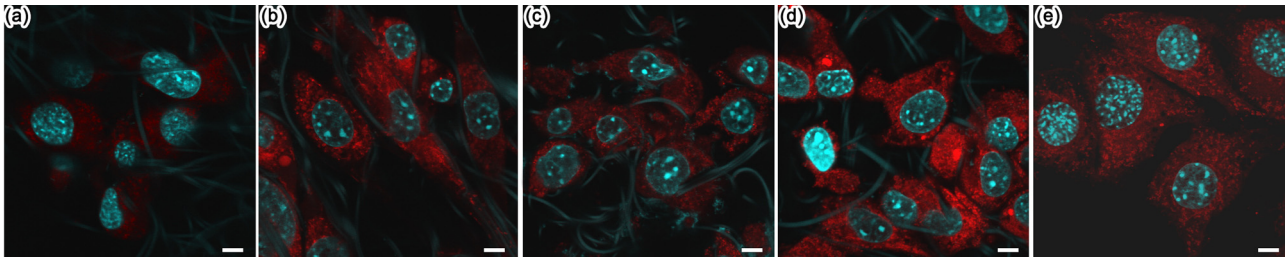

Fig. 6. Confocal images of NIH 3T3 cells seeded on the ternary composite NF membrane for (a) 1, (b) 3, (c) 5, and (d) 7 days and (e) glass coverslip stained with MitoTracker Red and DAPI. Scale bar: 10 μm.

3.7. Cell attachment and morphology

MitoTracker Red CMXRos is a cell-permeable vital dye that is taken up by mitochondria in response to the transmembrane potential across the inner mitochondrial membrane. Cells that lack an active mitochondrial transmembrane potential are unable to retain the dye (Geisler et al., 2010). Mitochondrial membrane potential is an indicator of cell health. Therefore, MitoTracker Red CMXRos staining reflects the healthy status of cells. DAPI staining is an established method for assaying cell viability and morphology of cell nuclei in cultured human cells. While normal cells show nuclei with a smooth and oval profile, cells undergoing apoptotic cell death reveal nuclear condensation and fragmentation (Galluzzi et al., 2009). As shown in Fig. 6, cells were seeded on the ternary membrane for 1, 3, 5 and 7 days, stained with MitoTracker Red CMXRos and DAPI, and were visualized with a confocal laser-scanning microscope. The morphology of the fibroblast cells is clearly visible. The mitochondria in the cytoplasm of cells are stained intensely by MitoTracker, and cell nuclei are clearly apparent, as in control cells grown on glass coverslips, indicating the cells are fully viable. It is observed that the fibroblast cells on the membrane cling to the fibers and use them as guides to grow. These results suggest that the ternary composite membranes are non-cytotoxic to fibroblast cells and cells can readily and effectively attach, spread and grow on these biocompatible nanofibrous membranes (Dubas, Kittitheeranun, Rangkupan, Sanchavanakit, & Potiyaraj, 2009; Jeong et al., 2013; Zhou et al., 2008). Strikingly, cells could permeate the membrane as early as the first day after seeding. Fig. 7 shows serial images moving the focal plane stepwise into the membrane after 3-day incubation, illustrating the migration of cells from the surface into the interior growing in between the fibers presumably by pushing through the fibrous structure. This suggests that the fibrous structure may thus enhance wound healing and assist faster re-epithelialization (Hartman et al., 2009). This also confirms that the pliability of the ternary membrane is not compromised. These membranes effectively mimic the natural extracellular matrix (ECM) in skin, offering a beneficial 3D environment for the fibroblast cells development while effectively preventing infections.

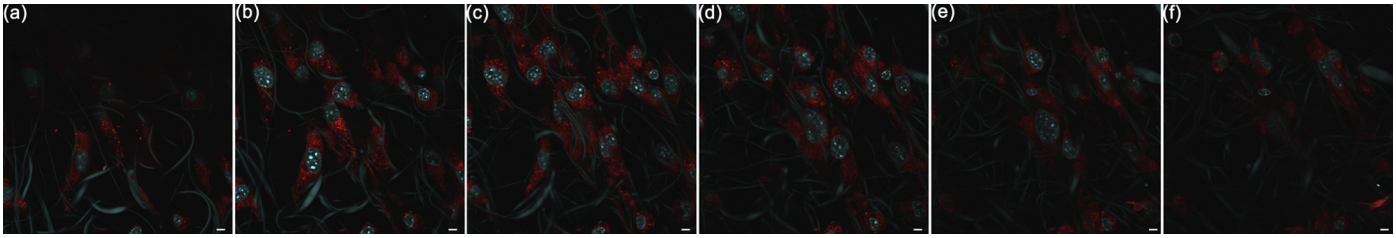

Fig. 7. Serial confocal images of NIH 3T3 cells seeded to ternary composite NF membrane followed by 3 days of incubation. Stepwise images were collected with focal plane = 1 μm. Scale bar: 10 μm.

4. Conclusions

Biocompatible TA/CS/PL composite NFs with synergistic antibacterial activity against the gram-negative bacteria *E. coli* and ability to promote cell attachment and growth were successfully mass produced from a CS-CA aqueous solution in the absence of organic solvents using forcespinning® method. The developed composite NFs are observed to be smooth, long and continuous. In order to ensure prolonged structural integrity for the wound dressing applications, the ternary composite nanofibrous membranes were effectively crosslinked by heat treatment, resulting in water stable membranes. The developed composites showed an effective and rapid water absorption capability, while also capable of holding water within the membrane, which greatly favors its use as wound dressing. Cell culture indicates that the developed antibacterial composite membranes are non-cytotoxic to NIH 3T3 fibroblast cells. These composite membranes effectively promote fibroblast cells attachment, and interlayer cells growth in an organized way of clinging to and along the fibers. These membranes also mimic the extracellular matrix (ECM) in skin and thus have the potential for the applications as wound dressing materials among others. The approach in this study could be applicable to produce NF membranes from other materials that have similar physicochemical properties for wound dressing applications. This study contributed to develop an understanding of the large-scale development of NF-based wound dressings from biocompatible materials using forcespinning® technology.

Conflict of interest

Dr. Lozano and The University of Texas - Pan American have research-related interest in FibeRio Technology Corporation.

Acknowledgements

This work was financially supported by National Science Foundation under DMR grant #0934157.

References

Aelenei, N., Popa, M. I., Novac, O., Lisa, G., & Balaita, L. (2009). Tannic acid incorporation in chitosan-based microparticles and in vitro controlled release. *Journal of Materials Science Materials in Medicine*, *20*, 1095–1102.

Azlan, K., Wan Saime, W. N., & Lai Ken, L. (2009). Chitosan and chemically modified chitosan beads for acid dyes sorption. *Journal of Environmental Sciences*, *21*, 296–302.

Baskar, D., & Sampath Kumar, T. S. (2009). Effect of deacetylation time on the preparation, properties and swelling behavior of chitosan films. *Carbohydrate Polymers*, *78*, 767–772.

Bolin, M. H., Karl Svennersten, K., Wang, X., Chronakis, I. S., Richter-Dahlfors, A., Jager, E. W. H., et al. (2009). Nano-fiber scaffold electrodes based on PEDOT for cell stimulation. *Sensors and Actuators B*, *142*, 451–456.

Can, M., Bulut, E., Örnek, A., & Özacar, M. (2013). Synthesis and characterization of valonea tannin resin and its interaction with palladium(II), rhodium(III) chloro complexes. *Chemical Engineering Journal*, *221*, 146–158.

Can, M., Bulut, E., & Özacar, M. (2012). Synthesis and characterization of gallic acid resin and its interaction with palladium(II), rhodium(III) chloro complexes. *Industrial and Engineering Chemistry Research*, *51*, 6052–6063.

Chen, Z., Mo, X., & Qing, F. (2007). Electrospinning of collagen–chitosan complex. *Materials Letters*, *61*, 3490–3494.

Cheng, K., Demirci, A., & Catchmark, J. M. (2010). Effects of plastic composite support and pH profiles on pullulan production in a biofilm reactor. *Applied Microbiology and Biotechnology*, *86*, 853–861.

Çolak, S. M., Yapici, B. M., & Yapici, A. N. (2010). Determination of antimicrobial activity of tannic acid in pickling process. *Romanian Biotechnological Letters*, *15*, 5325–5330.

de Abreu, F. R., & Campana-Filho, S. P. (2005). Preparation and characterization of carboxymethylchitosan. *Polímeros: Ciência e Tecnologia*, *15*, 79–83.

Desai, K., Kit, K., Li, J., & Zivanovic, S. (2008). Morphological and surface properties of electrospun chitosan nanofibers. *Biomacromolecules*, *9*, 1000–1006.

Dubas, S. T., Kittitheeranun, P., Rangkupan, R., Sanchavanakit, N., & Potiyaraj, P. (2009). Coating of polyelectrolyte multilayer thin films on nanofibrous scaffolds to improve cell adhesion. *Journal of Applied Polymer Science*, *114*, 1574–1579.

Galluzzi, L., Aaronson, S. A., Abrams, J., Alnemri, E. S., Andrews, D. W., Baehrecke, E. H., et al. (2009). Guidelines for the use and interpretation of assays for monitoring cell death in higher eukaryotes. *Cell Death and Differentiation*, *16*, 1093–1107.

Geisler, S., Holmström, K. M., Skujat, D., Fiesel, F. C., Rothfuss, O. C., Kahle, P. J., et al. (2010). PINK1/Parkin-mediated mitophagy is dependent on VDAC1 and p62/SQSTM1. *Nature Cell Biology*, *12*, 119–131.

Hang, A. T. (2010). E-spun mats of poly(vinyl alcohol)/chitosan blends containing silver nanoparticles: Fabrication and charachterization. *Carbohydrate Polymers*, *82*, 472–479.

Hartman, O., Zhang, C., Adams, E. L., Farach-Carson, M. C., Petrelli, N. J., Chase, B. D., et al. (2009). Microfabricated electrospun collagen membranes for 3-D cancer models and drug screening applications. *Biomacromolecules*, *10*, 2019–2032.

Helander, I. M., Lassila, E. L. N., Ahvenainen, R., Rhoades, J., & Roller, S. (2001). Chitosan disrupts the barrier properties of the outer membrane of Gram negative bacteria. *International Journal of Food Microbiology*, *71*, 235–244.

Ignatova, M., Starbova, K., Markova, N., Manolova, N., & Rashkov, I. (2006). Electrospun nano-fibre mats with antibacterial properties from quaternised chitosan and poly(vinyl alcohol). *Carbohydrate Research*, *341*, 2098–2107.

Jeong, H. G., Kim, Y. E., & Kim, Y. J. (2013). Fabrication of poly(vinyl acetate)/polysaccharide biocomposite nanofibrous membranes for tissue engineering. *Macromolecular Research*, *21*, 1233–1240.

Jia, Y., Gong, J., Gu, X., Kim, H., Dong, J., & Shen, X. (2007). Fabrication and characterization of poly (vinyl alcohol)/chitosan blend nanofibers produced by electrospinning method. *Carbohydrate Polymers*, *67*, 403–409.

Karim, M. R., Lee, H. W., Kim, R., Ji, B. C., Cho, J. W., Son, T. W., et al. (2009). Preparation and characterization of electrospun pullulan/montmorillonite nanofiber mats in aqueous solution. *Carbohydrate Polymers*, *78*, 336–342.

Kim, S., & Kim, H. J. (2003). Curing behavior and viscoelastic properties of pine and wattle tannin-based adhesives studied by dynamic mechanical thermal analysis and FT-IR-ATR spectroscopy. *Journal of Adhesion Science and Technology*, *17*, 1369–1383.

Kristo, E., Biliaderis, C. G., & Zampraka, A. (2007). Water vapour barrier and tensile properties of composite caseinate-pullulan films: Biopolymer composition effects and impact of beeswax lamination. *Food Chemistry*, *101*, 753–764.

Kumbar, S. G., James, R., Nukavarapu, S. P., & Laurencin, C. T. (2008). Electrospun nanofiber scaffolds: Engineering soft tissues. *Biomedical Materials*, *3*, 034002.

Li, H., Yang, J., Hu, X., Liang, J., Fan, Y., & Zhang, X. (2011). Superabsorbent polysaccharide hydrogels based on pullulan derivate as antibacterial release wound dressing. *Journal of Biomedical Materials Research Part A*, *98A*, 31–39.

Lozano K., Sarkar K. (2009). Methods and apparatuses for making superfine fibers. Patent 20090280325 A1, USA.

Mattioli-Belmonte, M., Zizzi, A., Lucarini, G., Giantomassi, F., Biagini, G., Tucci, G., et al. (2007). Chitin nanofibrils linked to chitosan glycolate as spray, gel and gauze preparations for wound repair. *Journal of Bioactive and Compatible Polymers*, *22*, 525–553.

McMurry, J. (2010). *Fundamentals of organic chemistry* (7th ed.). Belmont: Cengage Learning.

Min, B. M., Lee, G., Kim, S. H., Nam, Y. S., Lee, T. S., & Park, W. H. (2004). Electrospinning of silk fibroin nanofibers and its effect on the adhesion and spreading of normal human keratinocytes and fibroblasts in vitro. *Biomaterials*, *25*, 1289–1297.

Mohammed-Zieglera, I., & Billes, F. (2002). Vibrational spectroscopic calculations on pyrogallol and gallic acid. *Journal of Molecular Structure: THEOCHEM*, *618*, 259–265.

Muzzarelli, R. A. A. (2010). Chitins and chitosans as immunoadjuvants and non-allergenic drug carriers. *Marine Drugs*, *8*(2), 292–312.

Muzzarelli, R. A. A. (2012). Nanochitins and nanochitosans, paving the way to eco-friendly and energy-saving exploitation of marine resources. *Polymer Science: A Comprehensive Reference*, *10*, 153–164.

Muzzarelli, R. A. A., Boudrant, J., Meyer, D., Manno, N., DeMarchis, M., & Paoletti, M. G. (2012). Current views on fungal chitin/chitosan, human chitinases, food preservation, glucans, pectins and inulin: A tribute to Henri Braconnot, precursor of the carbohydrate polymers science, on the chitin bicentennial. *Carbohydrate Polymers*, *87*, 995–1012.

Muzzarelli, R. A. A., Tarsi, R., Filippini, O., Giovanetti, E., Biagini, G., & Varaldo, P. E. (1990). Antimicrobial properties of N-carboxybutyl chitosan. *Antimicrobial Agents and Chemotherapy*, *34*, 2019–2023.

Na, K., Shin, D., Yun, K., Park, K. H., & Lee, K. C. (2003). Conjugation of heparin into carboxylated pullulan derivatives as an extracellular matrix for endothelial cell culture. *Biotechnology Letters*, *25*, 381–385.

Ohkawa, K., Cha, D., Kim, H., Nishida, A., & Yamamoto, H. (2004). Electrospinning of chitosan. *Macromolecular Rapid Communications*, *25*, 1600–1605.

Padron, S., Fuentes, A., Caruntu, D., & Lozano, K. (2013). Experimental study of nanofiber production through forcespinning. *Journal Applied Physics*, *113*, 024318.

Padron, S., Patlan, R., Gutierrez, J., Santos, N., Eubanks, T., & Lozano, K. (2012). Production and characterization of hybrid BEH-PPV/PEO conjugated polymer nanofibers by forcespinning™. *Journal of Applied Polymer Science*, *125*, 3610–3616.

Pakravan, M., Heuzey, M. C., & Ajji, A. (2011). A fundamental study of chitosan/PEO electrospinning. *Polymer*, *52*, 4813–4824.

Paneva, D., Bougard, F., Manolova, N., Dubois, P., & Rashkov, I. (2008). Novel electrospun poly((-caprolactone)-based bicomponent nanofibers possessing surface enriched in tertiary amino groups. *European Polymer Journal*, *44*, 566–578.

Park, W. H., Jeong, L., Yoob, D. I., & Hudson, S. (2004). Effect of chitosan on morphology and conformation of electrospun silk fibroin nanofibers. *Polymer*, *45*, 7151–7157.

Pham, Q. P., Sharma, U., & Mikos, A. G. (2006). Electrospinning of polymeric nanofibers for tissue engineering applications: A review. *Tissue Engineering*, *12*, 1197–1211.

Qu, X., Wirsén, A., & Albertsson, A. C. (1999a). Structural change and swelling mechanism of pH-sensitive hydrogels based on chitosan and D,L-lactic acid. *Journal of Applied Polymer Science*, *74*, 3186–3192.

Qu, X., Wirsén, A., & Albertsson, A. C. (1999b). Synthesis and characterization of pH-sensitive hydrogels based on chitosan and D,L-lactic acid. *Journal of Applied Polymer Science*, *74*, 3193–3202.

Raghavan, B., Soto, H., & Lozano, K. (2013). Fabrication of melt spun polypropylene nanofibers by forcespinning. *Journal of Engineered Fibers and Fabrics*, *8*, 52–60.

Ramakrishna, S. (2005). *An introduction to electrospinning and nanofibers technology*. Singapore: World Scientific Publishing Co.

Ravi Kumar, M. N. V., Muzzarelli, R. A. A., Muzzarelli, C., Sashiwa, H., & Domb, A. J. (2004). Chitosan chemistry and pharmaceutical perspectives. *Chemical Reviews*, *104*, 6017–6084.

Rekha, M. R., & Sharma, C. P. (2009). Blood compatibility and *in vitro* transfection studies on cationically modified pullulan for liver cell targeted gene delivery. *Biomaterials*, *30*, 6655–6664.

Rieger, K. A., Birch, N. P., & Schiffman, J. D. (2013). Designing electrospun nanofiber mats to promote wound healing – A review. *Journal of Materials Chemistry B*, *1*, 4531–4541.

Rocasalbas, G., Touriño, S., Torres, J. L., & Tzanov, T. (2013). A new approach to produce plant antioxidant-loaded chitosan for modulating proteolytic environment and bacterial growth. *Journal of Materials Chemistry B*, *1*, 1241–1248.

Sarkar, K., Gomez, C., Zambrano, S., Ramirez, M., Hoyos, E., Vasquez, H., et al. (2010). Electrospinning to Forcespinning™. *Materials Today*, *13*, 12–14.

Scalbert, A. (1991). Antimicrobial properties of tannins. *Phytochemistry*, *30*, 3875–3883.

Shi, R., Bi, J., Zhang, Z., Zhu, A., Chen, D., Zhou, X., et al. (2008). The effect of citric acid on the structural properties and cytotoxicity of the polyvinyl alcohol/starch films when molding at high temperature. *Carbohydrate Polymers*, *74*, 763–770.

Singh, R. S., & Saini, G. K. (2007). Pullulan-hyperproducing color variant strain of *Aureobasidium pullulans* FB-1 newly isolated from phylloplane of *Ficus* sp. *Bioresource Technology*, *99*, 3896–3899.

Singh, R. S., Saini, G. K., & Kennedy, J. F. (2008). Pullulan: Mmicrobial sources, production and applications. *Carbohydrate Polymers*, *73*, 515–531.

Weng, B., Xu, F., Garza, G., Alcoutlabi sF M., Salinas, A., & Lozano, K. (2014). The Production of carbon nanotube reinforced poly(vinyl) butyral nanofibers by the Forcespinning® method. *Polymer Engineering and Science*, http://dx.doi.org/10.1002/pen.23872

Weng, B., Xu, F., & Lozano, K. (2014). Mass production of carbon nanotube-reinforced polyacrylonitrile fine composite fibers. *Journal of Applied Polymer Science*, *131*, 40302.

Weng, B., Xu, F., Salinas, A., & Lozano, K. (2014). Mass production of carbon nanotube reinforced poly(methyl methacrylate) nonwoven nanofiber mats. *Carbon*, http://dx.doi.org/10.1016/j.carbon.2014.03.056

Winter, G. D. (1962). Formation of the scab and the rate of epithelialization of superficial wounds in the skin of the young domestic pig. *Nature*, *193*, 293–294.

Xu, J., Zhang, J., Gao, W., Liang, H., Wang, H., & Li, J. (2009). Preparation of chitosan/PLA blend micro/nanofibers by electrospinning. *Materials Letters*, *63*, 658–660.

Yang, J., Webb, A. R., & Ameer, G. A. (2004). Novel Citric acid-based biodegradable elastomers for tissue engineering. *Advanced Materials*, *16*, 511–516.

Yuen, S. (1974). Pullulan and its applications. *Process Biochemistry*, *9*, 7–9.

Zahedi, P., Rezaeian, I., Ranaei-Siadat, S. O., Jafari, S. H., & Supaphol, P. (2010). A review on wound dressings with an emphasis on electrospun nanofibrous polymeric bandages. *Polymers for Advanced Technologies*, *21*, 77–95.

Zhou, Y., Yang, D., Chen, X., Xu, Q., Lu, F., & Nie, J. (2008). Electrospun water-soluble carboxyethyl chitosan/poly(vinyl alcohol) nanofibrous membrane as potential wound dressing for skin regeneration. *Biomacromolecules*, *9*, 349–354.